

EXPERIMENTAL STUDY OF NUCLEATE POOL BOILING WITH WATER IN ATMOSPHERIC PRESSURE

Onur AGMA^{*1,2}, Sebiha YILDIZ¹

¹ Yildiz Technical University, Faculty of Mechanical Engineering Department of Mechanical Engineering, Besiktas, Istanbul, Türkiye.

² Altinbas University, Faculty of Engineering and Architecture, Department of Mechanical Engineering, Bagcilar, Istanbul, Türkiye.

* Corresponding author; E-mail: onur.agma@altinbas.edu.tr

This study experimentally investigated nucleate pool boiling heat transfer for a polished copper surface and water fluid couple under atmospheric pressure. The results were compared with the correlations in the literature. The experimental results were compared with the surface-liquid correlation constants Rohsenow, Pioro, Vachon, Griffith and Das used for the temperature exceedance values. When the results of Griffith's correlation constant were compared with the experimental values, it was seen that it was the most appropriate correlation compared to other correlations, with a minimum and maximum error of 0.4-12%. In addition, Forster-Zuber, Pioro, Kutateladze old, Kutateladze new, Kruzhilin and Cooper correlations were compared with experimental results regarding the heat transfer coefficient. Compared with the correlation proposed by Pioro for the heat transfer coefficient, it was calculated as the most suitable correlation with a minimum and maximum difference of 0.2-8%.

Keywords: Nucleate pool boiling, water, polished copper, atmospheric pressure.

1. Introduction

Many known engineering applications include boiling heat transfer since heat transfer occurs at much higher rates than with single-phase fluids heat transfer. Boiling heat transfer is used in steam power plants, nuclear reactors, cooling of some electronic devices, etc. [1, 2]. Boiling is called pool boiling if there is no fluid mass movement and flow boiling if present. Boiling occurs at the solid-liquid interface as a result of the liquid coming into contact with a surface held at a temperature sufficiently higher than the saturation temperature [3]. Boiling begins with the formation of the first bubble. During the boiling process, the appearance of bubbles on the surface, the separation of steam bubbles from the surface and the filling of the separated steam bubbles by the fluid ensure the circulation of the fluid on the hot surface. In this process, which is called nucleate boiling, heat transfer increases with increasing surface temperature; this increase continues until the critical heat flux. Critical heat flux is a criterion related to system safety. For this reason, it is undesirable to exceed this limit state (critical heat flux) in most engineering applications. In this study, the correlations

available in the literature in the nucleate boiling section were compared with the experimental data and the correlations with the closest results to the experimental data were investigated.

Flow boiling differs from pool boiling due to the presence of liquid flow and the transportation of bubbles by this flowing liquid and there are many studies in the literature [4-6] on this subject. In addition, to flow boiling, there are many correlations in the literature [7] to calculate the heat transfer coefficient in nucleate pool boiling. With the help of these correlations, the heat transfer coefficient can be calculated without the need for challenging to calculate parameters such as bubble separation diameter and frequency [7]. Das et al. [8] calculated the error rates by comparing different correlations with their experimental heat transfer coefficient using copper-water pair and revealed that the Rohsenow correlation matched at the lowest error rate. Choon et al. [9] conducted an experimental study using copper foam surface-water under the effect of low pressure and they suggested that the surface temperature difference value could be calculated with the modified Rohsenow correlation. Gao et al., in their study [10] on copper–water couple, stated that the experimental study was confirmed by the Rohsenow correlation in terms of heat flux and surface temperature difference. Yao et al. [11] carried out experiments with water by coating nanoparticles on the copper foam surface and used the Rohsenow correlation for heat transfer estimation and suggested a correction coefficient for the copper foam surface in this study. In their study [12], Pezo and Stevanovic estimated the nucleate boiling heat transfer coefficient at high heat flux using numerical simulation and compared this estimation with the correlations of Mostinski, Rohsenow, Kutateladze old, Kutateladze new, and Kruzhilin. They emphasized the importance of surface roughness. The closest numerical results are Kruzhilin and new Kutateladze correlations on aged surfaces and Mostinski and old Kutateladze correlations on fresh surfaces. In the study of Haji et al. [13], which is one of the studies on changing the surface roughness, comparisons were made with the experimental results using the correlations of Rohsenow, Cooper and Gornflow on the uncoated surface. In the study of Theofanous et al. [14], both fresh heaters and aged heaters were experimented. They used a high-speed, high-resolution infrared camera to visualize dynamic thermal patterns from the onset of nucleation to boiling crisis. They found a difference in nucleation patterns between the fresh and aged heaters. They reported that the surface average wall superheat at the critical heat flux varied from 22 to 32 K on fresh heaters and from 18 to 25 K on aged heaters. They also carried out experiments on critical heat flux using fresh and aged heaters [15].

Surface-fluid couple is one of the critical parameters affecting heat transfer in pool boiling. Heat transfer can be improved by changing the surface material and the roughness of the surface [16-20]. Another important factor affecting heat transfer is changing the properties of the liquid, such as the use of nanofluids [21-24].

Heat transfer mechanisms are pretty complex in boiling and many correlations exist in the literature [7]. In the literature, the Rohsenow correlation (equation 1) is widely used in nucleate boiling [25, 26].

$$C_{pl}\Delta T_{sat}/h_{fg} = C_{sf} \left\{ (\dot{q}/\mu_l h_{fg})(\sigma g_c/g(\rho_l - \rho_g))^{0.5} \right\}^r [C_{pl}\mu_l/k_l]^n \quad (1)$$

Here C_{sf} is a constant that depends on the liquid and the surface coating. The surface-fluid pair used in this study is polished copper and water. The different C_{sf} and n values suggested in the literature for the polished copper and water surfactant couple are presented in Table 1.

Table 1. C_{sf} and n values for water and polished copper pair in the literature.

Reference	C_{sf}	n
Rohsenow [27]	0.0130	1
Pioro 1999 [28]	0.0150	0.81
Vachon 1968 [29]	0.0142	1
Griffith 1960 [29]*	0.0147	1
Das 2007 [30]	0.0160	1

* The coefficients proposed by Griffith are taken from reference [29].

Pioro [28] conducted experimental studies to determine the C_{sf} and n coefficients. Based on the experimental results, he suggested the C_{sf} and n values as 0.015 and 0.81, respectively, and reported that they remained within the error range of $\pm 25\%$ when comparing the experimental and correlation values. Vachon et al. [29] suggested the n value as 1 for water. C_{sf} values were calculated using the least squares curve fitting technique for the heat flux and temperature exceedance values obtained using different surface-fluid pairs from the literature. The results are presented in tables. In that study [29], they suggested a C_{sf} coefficient of 0.0142 for the surface-fluid couple of the copper surface and water polished with sandpaper. In the same study, they reported the C_{sf} coefficient suggested by Griffith as 0.0147. In the study of Das et al. [30], the C_{sf} coefficient for the copper surface and water, which has 600 μm gaps at different points, was accepted as 0.0160 and compared with the experimental values. The C_{sf} and n coefficients presented in Table 1 were substituted in the correlation suggested by Rohsenow and the results were compared in section 3.

Different correlations exist in the literature [7] to determine the heat transfer coefficient in nucleate pool boiling. The correlations presented in Table 2 have been utilized in this study.

Forster and Zuber [25, 31] suggested the correlation shown in equation (2) for the calculation of the heat transfer coefficient. In addition to this correlation fluid properties and temperature excess, the difference between the fluid saturation pressure at the surface temperature and the saturation pressure at the saturation temperature of the fluid is considered. However, this correlation does not consider the effect of the surface-fluid couple.

Pioro et al. [28] reported conducting studies to evaluate Rohsenow's correlation constants empirically. Some suggestions for C_{sf} and n coefficients were made by this group considering different surfactant pairs [32]. Instead of the coefficients in the Rohsenow correlation, they used the C_{sf}^* and m coefficients in their proposed correlation for the heat transfer coefficient calculation. They suggested C_{sf}^* and m values as 1228 and -1.1, respectively, for the water-copper surface fluid couple [32]. In this study, the heat transfer coefficient was calculated using the coefficients suggested above. In addition, as seen in equation (3), the experimental heat flux values have been used to calculate the heat transfer coefficient.

In their work, Pioro et al. [32] shared Kutateladze's so-called old and new correlations and Kruzhilin correlation. These correlations are shown in equations (4), (5) and (6) as Kutateladze old, new and Kruzhilin correlations, respectively [32]. Equation (5), which Kutateladze called new, includes the coefficient given as M^* . In the Kruzhilin correlation shown in equation (6), the calculation is made using the experimental heat flux value.

Apart from these correlations, there are also some suggested correlations by considering the surface roughness and using the pressure values. Among these correlations, the equation (7) proposed by Cooper was also used in this study [33]. The C value in the correlation varies with the surface material and is suggested as 95 for horizontal copper surfaces [34].

Table 2. Nucleate Pool-boiling Heat Transfer Correlations.

Author	Correlation	Eq. Number
Rohsenow [27]	$\dot{q} = \mu_l h_{fg} [g(\rho_l - \rho_v)/\sigma]^{1/2} \left[(C_{pl}(T_s - T_{sat})) / (C_{sf} h_{fg} Pr_l^n) \right]^3$	(1)
Forster-Zuber [25]	$h = 0.00122 \Delta T_{sat}^{0.24} \Delta P_{sat}^{0.75} c_{pl}^{0.45} \rho_l^{0.49} k_l^{0.79} / \sigma^{0.5} h_{fg}^{0.24} \mu_l^{0.29} \rho_g^{0.24}$	(2)
Pioro [32]	$h_b l_*/k = C_{sf}^* \left\{ \dot{q} / (h_{fg} \rho_g^{0.5} [\sigma g(\rho - \rho_g)]^{0.25}) \right\}^{2/3} Pr^m$	(3)
Kutateladze old [32]	$h_b l_*/k = 0.44 \left((1 \times 10^{-4} \dot{q} p / g h_{fg} \rho_g \mu) (\rho / \rho - \rho_g) \right)^{0.7} Pr^{0.35}$	(4)
Kutateladze new [32]	$M_*^4 = \frac{\sigma g}{\left(\frac{p - p_s}{\rho_g} \right)^2} \quad h_b = \left[3.37 \times 10^{-9} (k/l_*) (h_{fg}/c_{pl} \dot{q})^{-2} M_*^{-4} \right]^{1/3}$	(5)
Kruzhilin [32]	$h_b l_*/k = 0.082 \left((h_{fg} \dot{q} / g (T_{sat} + 273.15) k) (\rho / \rho - \rho_g) \right)^{0.7} \left((T_{sat} + 273.15) c_{pl} \sigma \rho / h_{fg}^2 \rho_g^2 l_* \right)^{0.33} Pr^{-0.45}$	(6)
Cooper [33]	$h = C (Pr^{0.12 - 0.2 \log_{10} Ra}) (-\log_{10} Pr)^{-0.55} M^{-0.5} \dot{q}^{0.67}$ C=95 for horizontal copper surface	(7)

In this study, the experimentally measured surface temperature exceedance values were compared with the temperature exceedance values obtained from the Rohsenow correlation calculated with different C_{sf} values. In addition, the heat transfer coefficient was obtained experimentally and compared with Forster-Zuber, Pioro, Kutateladze (old and new), Kruzhilin, Cooper correlations. The correlations are in the same range as the measured data.

Studies in the literature have generally been carried out in areas close to the critical heat flux where bubbles occur intensely. This study focused on the 'isolated bubble regime' region at low heat fluxes, starting from the first bubble formation in pool boiling. The correlations available in the literature and the experimental results were compared for this region and the correlations that provided the closest results to the experimental data were searched. Thus, appropriate correlations from the literature can be suggested for the 'isolated bubble regime' region.

2. Experimental Setup and Method

The experimental setup consists of seven main components: (1) the copper block used as the heating surface, (2) the boiling vessel in which the liquid is kept, (3) the condensation system that allows the evaporating liquid to return to the system, (4) the power control system in which the heater can be controlled, (5) thermocouples for measuring temperature values, (6) data acquisition system and (7) insulation. The schematic of the pool boiling experimental setup is shown in Figure 1.

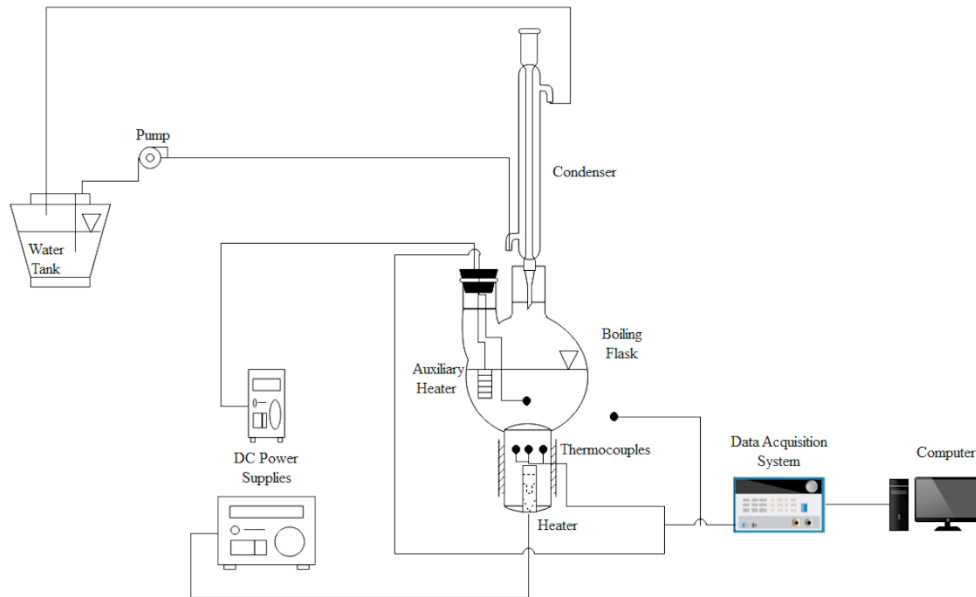


Figure 1. Scheme of the experimental setup.

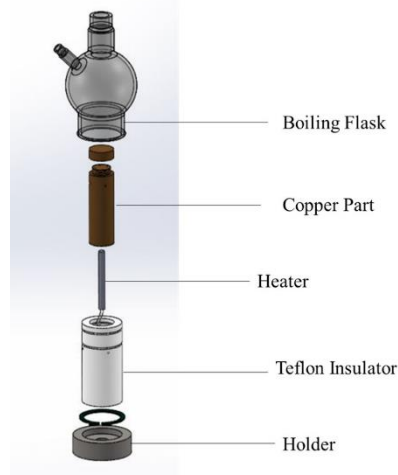


Figure 2. An exploded view of the section containing the heating surface, the boiling flask and the heater.

As seen in Figure 2, the copper block has a diameter of 40 mm and it was heated by a cartridge heater (500 W). The pure copper block transfers the given heat to the surface and acts as a boiling surface where the heat is transferred to the working fluid. In this part of the experimental setup, the upper side of the copper block was designed as replaceable and produced in bolt-nut connection type. This connection and heater location are shown in detail in Figure 3. In order to measure the temperatures on the surface and calculate the heat flux transferred to the fluid, eight holes (2.5 mm)

were drilled in different places in the copper block. Five of these holes are placed to measure temperature from different parts of the surface in contact with water. To determine the temperature of the surface where the boiling takes place, four holes (T1, T4, T5, T8) were drilled at a distance of 10 mm from the middle and 90° between them. There is a hole located 25 mm (T3) below the surface of the middle section to determine the vertical heat flux (Section B-B).

Section A-A shows that one is T6, which is on the same vertical axis and 25 mm below the hole called T5, and the other is T7, located 5.5 mm below the T6 hole. The locations of these holes are shown in detail in Figure 3. Temperature measurements were carried out by placing K-type thermocouples in the holes.

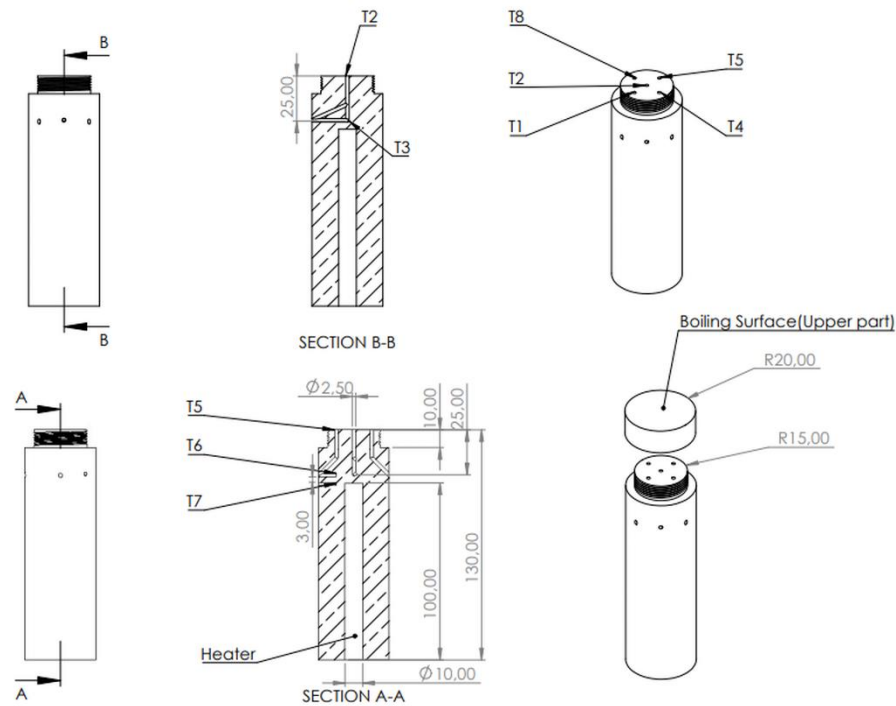


Figure 3. Copper block, boiling surface (cover), thermocouple connection channels and places.

Borosilicate glass 1000 mL 2-necked balloon flask boiling flask is produced with an open bottom to be placed on the copper block. There are two necks on the upper side of the boiling flask. A 40 cm long borosilicate glass dimroth condenser is placed in one of them. On the other neck, both a thermocouple is inserted to measure the temperature of the water and an auxiliary cartridge heater (30W) used to heat the water externally is immersed. Water circulation in the condenser is provided from the water tank at ambient temperature with the help of a pump.

A DC power source operates the cartridge heater inside the copper block. Data were recorded when there was no change in boiling surface temperature to ensure steady state heat transfer.

In addition, there is a data acquisition system, K-type thermocouples, PT100 and a computer in the experiment facility. Thermocouples and cartridge heater were placed inside the copper block, while the thermal paste was used to fill all the gaps. The copper block is insulated with 12.5 mm thick Teflon material. Additional insulation was made with glass wool on the outside of the Teflon. The copper block is wholly covered with Teflon and placed on the gas concrete block. The boiling pot is insulated against the environment with glass wool. A small observation area is left to observe the boiling. This study used ultrapure water (15 MΩ.cm) as the fluid.

2.1. Heated Surface

After being brought to the required geometry, copper, selected as the heating surface, was initially polished using a grinding machine (Metkon Forcimat) with 1000-grit sandpaper (Hermes WS Flex) at 150 rotations per minute to remove any lathe marks. Then, the surface was polished with 1200 sandpaper (Hermes WS Flex) at 150 rpm. The surface roughness value was measured with a device called Mahr Marsurf PS1. In Figure 4, the places where the measurements were made are shown schematically. The average surface roughness value was measured as R_a (μm) and is presented in Table 3.

Table 3. Surface Roughness.

Surface Properties			
Material	Thermal Conductivity	Roughness R_a (μm)	Diameter (mm)
Copper	400 W/mK	0.122	40
		0.100	
		0.091	
		0.107	
		0.109	
		0.091	

The average surface roughness (R_a) value was obtained as 0.103 μm . Considering this value, the copper surface is considered polished [8].



Figure 4. Surface roughness measurement and schematic representation of the measurement paths.

2.2. Test Procedure

Before starting the experiments, the water level in the boiling vessel was checked. Before starting the main heater in the copper block, the submerged auxiliary heater is operated with 12 W power and preheated to the water. Then the cartridge heater in the copper block is operated with 20 W power. When evaporation starts, the cold-water circulation pump circulating in the condenser is started and the adjusted heater power is waited until the pure water saturation temperature is reached. Then, by increasing the heater power, it waits until the temperature values measured on the surface remain unchanged in the initial state of boiling. The first data started to be recorded approximately 4 hours after the start of the experimental setup. Later, the heater powers were increased with small steps. After each power increase, it was waited for at least 30 minutes for the temperature values to be stable.

All thermocouples with PT100 (Fluke 5626) with a measurement uncertainty of ± 0.05 at $100\text{ }^{\circ}\text{C}$ were placed in the calibration furnace and calibrated at $50\text{-}150\text{ }^{\circ}\text{C}$.

2.3. Analysis of Uncertainty and Error Rate Calculations

The calculated heat flux and the uncertainty in the heat transfer coefficient were determined using the Moffat [35] method. The uncertainty in this study is mainly due to the accuracy of the temperature values measured by the thermocouples and the calipers for length measurement.

The measurement error of K-type thermocouples is about $\pm 0.05\text{ }^{\circ}\text{C}$. Manufacturing tolerances on hole diameters are estimated as $\pm 0.05\text{ mm}$. The precision value of the caliper used for distance measurements is $\pm 0.03\text{ mm}$. It is known that deviations of up to $6\text{ }\mu\text{V}$ can occur in the data acquisition system used. The uncertainties in the heat flux and heat transfer coefficient calculated for the tested fluid were 11% and 12%, respectively, according to the Moffat [35] method.

Error calculations are presented to compare the temperature exceedance values and the heat transfer coefficient values determined by correlations with the experimental results. First, the error calculation (8) is specified in the equation.

$$\text{Error} = (\text{Calculated Value} - \text{Experimental Value}) / \text{Experimental Value} \quad (8)$$

Error values calculated from here and mean error and root mean square errors were calculated according to equations (9) and (10), respectively.

$$\text{Mean Error} = \sum_{i=1}^n \text{Error}_i / n \quad (9)$$

$$\text{Root Mean Square Error} = \left(\sum_{i=1}^n \text{Error}_i^2 / n \right)^{1/2} \quad (10)$$

3. Results and Discussion

Considering the temperature difference and the vertical distance difference (25 mm) at points 2 and 3 shown in Figure 3 (section B-B), the heat flux calculation was made according to equation (11). Here, the heat transfer coefficient for the copper block is taken as $400\text{ Wm}^{-1}\text{K}^{-1}$.

$$\dot{q} = k (T_3 - T_2) / L_{2-3} \quad (11)$$

3.1. Comparison of experimental temperature exceedance values with correlations

The temperature at the center of the boiling surface was obtained by equation (12) with the assumption of constant heat flux from the T2 point on the vertical center axis of the copper block to the boiling surface ($L_{2-s} = 5\text{ mm}$).

$$T_s = T_2 - ((T_3 - T_2)L_{2-s} / L_{2-3}) \quad (12)$$

Nucleate boiling experiments with water were repeated on different days and the same results were obtained.

While calculating the heat flux with the Rohsenow equation when the temperature exceedance is known, errors of up to 100% may occur, while in the case of calculating the temperature difference for a known heat flux ($\Delta T_s \propto (\dot{q})^{1/3}$), the error rate is reduced by 3 times [27]. For this reason, the Rohsenow equation (13) was used in this study to calculate the temperature difference values based on the experimentally obtained heat fluxes.

$$\dot{q} = \mu_l h_{fg} [g(\rho_l - \rho_v) / \sigma]^{1/2} \left[\left(C_{pl}(T_s - T_{sat}) \right) / (C_{sf} h_{fg} Pr_l^n) \right]^3 \quad (13)$$

Considering that the roughness level obtained was $0.103\text{ }\mu\text{m}$, the surface used was accepted as a polished copper surface. For the polished copper-water couple, the C_{sf} coefficient in the Rohsenow

equation is 0.0130 and the n value is 1 [27]. However, different C_{sf} and n values are suggested in the literature for the polished copper-water couple, these values are presented in Table 1.

Figure 5 shows the comparison of the experimental values and the temperature difference values obtained from the correlations. The maximum and minimum differences between the values calculated according to the experimental values are shown in Table 4. When considering the obtained error values, the maximum error calculated using the Griffith 1960 [29] correlation was found to be 12%, which is lower than the other correlations.

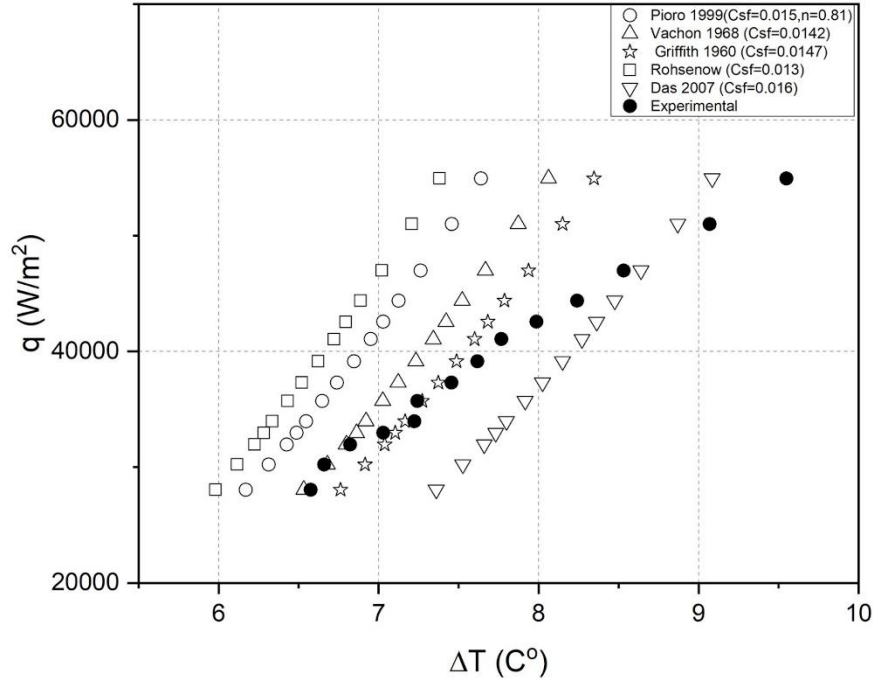


Figure 5. Comparison of experimental temperature difference values with correlations.

Table 4. The values of the excess temperature according to Rohsenow, their maximum, minimum, mean and RMS error values.

Reference	C_{sf}	n	Maximum Error %	Minimum Error %	Mean Error (%)	RMS Error (%)
Rohsenow [27]	0.0130	1	21	8	-13.69	14.32
Pioro 1999 [28]	0.0150	0.81	20	5	-10.78	11.59
Vachon 1968 [29]	0.0142	1	16	0.3	-5.72	7.34
Griffith 1960 [29]	0.0147	1	12	0.4	-2.4	5.33
Das 2007 [30]	0.0160	1	13	1	6.23	8.11

First, the mean error and root mean square (RMS) error values according to the Rohsenow equation calculated with different C_{sf} values for temperature exceedance values are shown in Table 4.

When the error rates presented in Table 4 are examined, it is seen that the mean error value for the temperature exceedance value calculated by taking the C_{sf} coefficient suggested by Griffith as 0.0147 is the lowest. In addition, it is seen that all mean error and RMS values in Table 4 are within acceptable values.

3.2. Comparison of heat transfer coefficient with correlations

Figure 6 shows the comparison of the test results in terms of heat transfer coefficients with the different correlations presented in Table 2. The heat transfer coefficient was found by substituting the experimentally obtained heat flux in equation (14).

$$h = \dot{q} / \Delta T \quad (14)$$

Experimental heat transfer coefficients and maximum and minimum error values of the results calculated with the correlations in Table 2 are presented in Table 5.

When the experimentally obtained heat transfer coefficient and Forster-Zuber correlation (3) were compared, it was seen that the values with the lowest and highest error rates were 2-28%. Since the relationship between the fluid and the boiling surface are not taken into consideration in this correlation, it can be interpreted as an expected result that it has the highest error rate.

Kutateladze old (4) and Kutateladze new (5) correlations are also used in the literature [32] and shown in Table 2. It is seen that the heat transfer coefficient calculated with the equation (5), which is called new from these correlations, gives results between 3-21% error rates according to the experimental results. In Kutateladze's correlation number (4), which is called old, it has been revealed that it has error rates in the range of 17-31%.

The calculations performed using equation (6), which is based on Kruzhilin correlation [32], exhibit error rates ranging from 0.1 to 14% compared to the experimental results. Table 5 shows that although the maximum error of this correlation is higher than the Pioro (3) correlation, it is lower than the other correlations.

The Pioro correlation [32] is the closest correlation to the experimentally obtained heat transfer coefficient values. Here, the minimum and maximum error value is between 0.2-9%.

Finally, when examining the Cooper correlation [33] represented by the proposed equation (7) based on surface roughness, it is observed to have a significantly higher error range of 25-40% compared to the error values of other correlations.

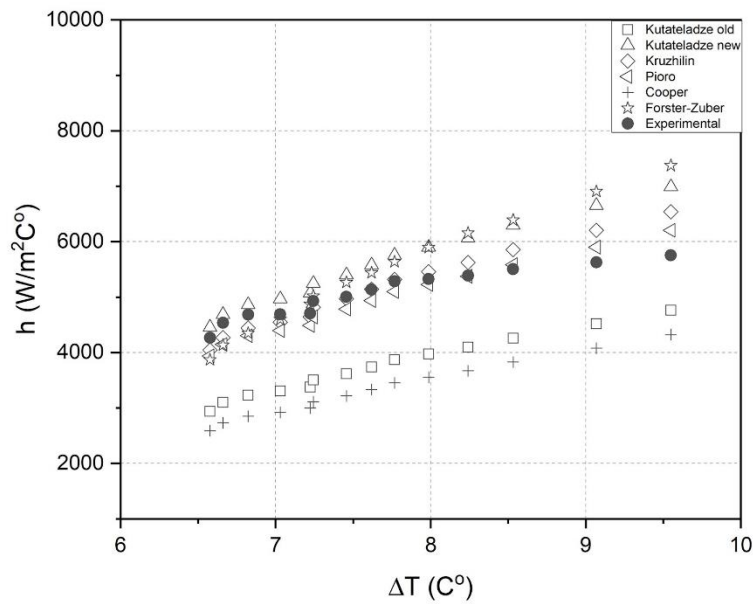


Figure 6. Comparison of heat transfer coefficients with different correlations (HTC).

Table 5. Comparison of the calculated heat transfer coefficient from the correlations with experimental results, including maximum, minimum, mean and RMS error.

Author [Ref]	Maximum Error %	Minimum Error %	Mean Error %	RMS Error %
Forster-Zuber [25]	28	2	6.28	12.62
Pioro [32]	9	0.2	-2.92	5.55
Kutateladze old [32]	31	17	-26.53	26.84
Kutateladze new [32]	21	3	9.63	10.94
Kruzhilin [32]	14	0.1	1.05	5.75
Cooper [33]	40	25	-34.46	34.72

Correlations were compared with experimental results and presented in Table 5. As a result, the minimum and maximum error rates of the correlations calculated with the experimentally obtained heat transfer coefficient values were revealed. When these error rates are compared, it can be considered that error rates are acceptable in all other correlations except for equation (4) and Cooper (equation (7)), which is called the Kutateladze old.

The mean error and RMS error values calculated for the heat transfer coefficient correlations are shown in Table 5. According to the values obtained in Table 5, it can be observed that the Kruzhilin and Pioro correlations can predict the experimental data with minimal error.

4. Conclusions

In this study, heat transfer was investigated experimentally in the region of discrete bubble formation of bubbles in nucleate pool boiling for a polished copper-water fluid couple at atmospheric pressure. The experiment results are evaluated in terms of temperature exceedance values and heat transfer coefficient and compared with the correlations available in the literature.

- Experimental results were compared with Rohsenow, Pioro, Vachon, Griffith and Das correlations for temperature exceedance values. When the Griffith correlation results were compared with the experimental values, the minimum and maximum error of 0.4-12% was found to be the most appropriate correlation compared to other correlations.
- For the heat transfer coefficient, Forster-Zuber, Pioro, Kutateladze old, Kutateladze new, Kruzhilin and Cooper correlations were compared with the experimental results. In terms of heat transfer coefficient, the correlation suggested by Pioro was found to be the most appropriate correlation with a minimum and maximum difference of 0.2-8% when compared with the experimental results.

This experimental study can assist in determining the temperature exceedance at the same heat flux for the polished copper-water surface fluid couple in pool boiling at atmospheric pressure, and in choosing the appropriate correlation for calculating the heat transfer coefficient.

Acknowledgement

The authors would like to thank Alarge Ltd. Co. for their support during the experimental research. This study is based on a part of Ph.D. dissertation at Yıldız Technical University.

Nomenclature

C_{pl}	specific heat [$\text{J kg}^{-1} \text{K}^{-1}$]
C_{sf}	coefficient of Rohsenow correlation (Eq. 2)
C_{sf}^*	coefficient of Piro correlation (Eq.3)
g	acceleration due to gravity [m s^{-2}]
g_c	gravitational constant (for imperial unit)
h	heat transfer coefficient [$\text{W m}^{-2} \text{K}^{-1}$]
h_{fg}	latent heat of vaporization [J kg^{-1}]
k	thermal conductivity [$\text{W m}^{-1} \text{K}^{-1}$]
L	Length [m]
l^*	pool boiling characteristic dimension, $\left[\frac{\sigma}{g(\rho - \rho_g)} \right]^{0.5}$ [m]
M	Molecular weight
p	pressure [Pa]

P_r	reduced pressure [Pa]
R_a	arithmetic-average roughness
\dot{q}	heat flux [W m^{-2}]
T	temperature [$^{\circ}\text{C}$]
T_s	surface temperature

Greek Symbols

Δ	difference
μ	dynamic viscosity [Pa s]
ρ	density [kg m^{-3}]
σ	surface tension [N m^{-1}]
ν	kinematic viscosity $\left[\frac{\mu}{\rho} \right]$ [$\text{m}^2 \text{s}^{-1}$]

Subscripts

b	boiling
c	condensation
cr	critical
f	saturated fluid
g	saturated vapor
l	liquid
p	at constant pressure
sat	saturation
sf	surface-fluid
v	saturated vapor

Non-dimensional numbers

Pr	Prandtl number $\frac{c_p \mu}{k}$
------	------------------------------------

Abbreviations

HTC	heat transfer coefficient
-----	---------------------------

Note: Physical properties with no subscript refer to saturated liquid.

References

- [1] Dahariya, S., Betz, A. R., High pressure pool boiling: Mechanisms for heat transfer enhancement and comparison to existing models, *Int. J. Heat Mass Transf.*, 141 (2019), pp. 696–706, doi: 10.1016/j.ijheatmasstransfer.2019.07.016.
- [2] Balaji C., et. al., *Heat transfer engineering: fundamentals and techniques*, Academic Press, London, England, 2021.
- [3] Kandlikar, S. G., *Handbook of Phase Change: Boiling and Condensation*, Taylor&Francis, Philadelphia, USA, 2019.
- [4] Yildiz, S., Effect of length-to-diameter ratio on critical heat flux in porous-coated tubes, *Thermal Science*, 25, (2021), 1 Part B, pp. 613–623, doi: 10.2298/TSCI190426462Y.
- [5] Guo, J. et. al., Experimental study on boiling heat transfer in negative-pressure flowing water in a vertical annular tube, *Thermal Science*, 26, (2022), 6 part B, pp. 5121–5129, doi: 10.2298/TSCI220224093G.
- [6] Jing, Q., Luo, Q., Experimental study on the correlation of subcooled boiling flow in horizontal tubes, *Thermal Science*, 26, (2022), no. 1 Part A, pp. 107–117, doi: 10.2298/TSCI200801339J.
- [7] Guichet V., et. al., Nucleate pool boiling heat transfer in wickless heat pipes (two-phase closed thermosyphons): A critical review of correlations, *Therm. Sci. Eng. Prog.*, 13, (2019), 100384, doi: 10.1016/j.tsep.2019.100384.
- [8] Das, S., et. al., Experimental study of nucleate pool boiling heat transfer of water by surface functionalization with crystalline TiO₂ nanostructure, *Appl. Therm. Eng.*, 113, (2017), pp. 1345–1357, doi: 10.1016/j.applthermaleng.2016.11.135.
- [9] Choon, N. K. et. al., New pool boiling data for water with copper-foam metal at sub-atmospheric pressures: Experiments and correlation, *Appl. Therm. Eng.*, 26, (2006), 11–12, pp. 1286–1290, Aug. 2006, doi: 10.1016/j.applthermaleng.2005.10.028.
- [10] Gao, L., et al., Experimental studies for the combined effects of micro-cavity and surface wettability on saturated pool boiling, *Exp. Therm. Fluid Sci.*, 140, (2023), 110769, doi: 10.1016/j.expthermflusci.2022.110769.
- [11] Yao, H., et. al., Modification and pool boiling performance elevation of copper foam wicks for high power applications, *Appl. Therm. Eng.*, 220, (2023), 119788, doi: 10.1016/j.applthermaleng.2022.119788.
- [12] Pezo, M. L., Stevanovic, V. D., Numerical prediction of nucleate pool boiling heat transfer coefficient under high heat fluxes, *Thermal Science*, 20, (2016), pp. 113-123, <http://dx.doi.org/10.2298/TSCI150701138P>.
- [13] Haji, A., et. al., Enhanced boiling heat transfer efficiency through the simultaneous use of electrospray and photolithography methods: An experimental study and correlation, *Therm. Sci. Eng. Prog.*, 38, (2023), 101661, doi: 10.1016/j.tsep.2023.101661.

- [14] Theofanous, T. G., Tu, J. P., Dinh, A.T., Dinh, T.N. The boiling crisis phenomenon Part I: nucleation and nucleate boiling heat transfer, *Experimental Thermal and Fluid Science*, 26, (2002), pp. 775–792, [https://doi.org/10.1016/S0894-1777\(02\)00192-9](https://doi.org/10.1016/S0894-1777(02)00192-9).
- [15] Theofanous, T. G., Tu, J. P., Dinh, A.T., Dinh, T.N. The boiling crisis phenomenon Part II: dryout dynamics and burnout, *Experimental Thermal and Fluid Science*, 26, (2002), pp. 793–810, [https://doi.org/10.1016/S0894-1777\(02\)00193-0](https://doi.org/10.1016/S0894-1777(02)00193-0).
- [16] Jo, H., et. al., A study of nucleate boiling heat transfer on hydrophilic, hydrophobic and heterogeneous wetting surfaces, *Int. J. Heat Mass Transf.*, 54, (2011), 25–26, pp. 5643–5652, doi: 10.1016/j.ijheatmasstransfer.2011.06.001.
- [17] Wen, D., et. al., Boiling heat transfer of nanofluids: The effect of heating surface modification, *Int. J. Therm. Sci.*, 50, (2011), 4, pp. 480–485, doi: 10.1016/j.ijthermalsci.2010.10.017.
- [18] Cooke, D., Kandlikar, S. G., Effect of open microchannel geometry on pool boiling enhancement, *Int. J. Heat Mass Transf.*, 55, (2012), 4, pp. 1004–1013, doi: 10.1016/j.ijheatmasstransfer.2011.10.010.
- [19] Sarangi, S., et. al., Effect of particle size on surface-coating enhancement of pool boiling heat transfer, *Int. J. Heat Mass Transf.*, 81, (2015), pp. 103–113, doi: 10.1016/j.ijheatmasstransfer.2014.09.052.
- [20] Thangavelu, N., et. al., Influence of surface roughness and Wettability of novel surface on nucleate boiling performance in deionised water at atmospheric pressure, *Thermal Science.*, 26, (2022), 6 Part A, pp. 4645–4656, doi: 10.2298/TSCI211202062T.
- [21] Kathiravan, R. et. al., Preparation and pool boiling characteristics of copper nanofluids over a flat plate heater, *Int. J. Heat Mass Transf.*, 53, (2010), 9–10, pp. 1673–1681, doi: 10.1016/j.ijheatmasstransfer.2010.01.022.
- [22] Xuan, Y., Li, Q., Heat transfer enhancement of nanofluids, *International Journal of Heat and Fluid Flow*, 21, (2000), pp. 58–64.
- [23] Park K. J., Jung, D., Enhancement of nucleate boiling heat transfer using carbon nanotubes, *Int. J. Heat Mass Transf.*, 50, (2007), 21–22, pp. 4499–4502, doi: 10.1016/j.ijheatmasstransfer.2007.03.012.
- [24] Ali, H. M., et. al., Experimental investigation of nucleate pool boiling heat transfer enhancement of TiO₂-water based nanofluids, *Appl. Therm. Eng.*, 113, (2017), pp. 1146–1151, doi: 10.1016/j.applthermaleng.2016.11.127.
- [25] Rohsenow, W. M., et. al., *Handbook of heat transfer*, McGraw-Hill, New York, USA, 1998.
- [26] Rohsenow, W.M., A Method of Correlating Heat Transfer Data for Surface Boiling of Liquids, Report No. 5, MIT, Cambridge, USA, 1951.
- [27] Cengel, Y. A., et. al., *Isı ve Kütle Transferi Pratik bir Yaklaşım* (Heat and Mass Transfer A Pratical Approach), Güven Kitabevi, İstanbul, Türkiye, 2011 (in Turkish language).
- [28] Piro, I. L., Experimental evaluation of constants for the Rohsenow pool boiling correlation, *Int. J. Heat Mass Transf.*, 42, (1999), 11, pp. 2003–2013, doi: 10.1016/S0017-9310(98)00294-4.

- [29]Vachon, R. I., Evaluation of Constants for the Rohsenow Pool-Boiling Correlation, *J. Heat Transf.*, 90, (1968), 2, pp. 239–246, doi: 10.1115/1.3597489.
- [30]Das, A. K., et.al., Nucleate boiling of water from plain and structured surfaces, *Exp. Therm. Fluid Sci.*, 31, (2007), 8, pp. 967–977, doi: 10.1016/j.expthermflusci.2006.10.006.
- [31]Forster, H. K., Zuber, N., Dynamics of vapor bubbles and boiling heat transfer, *AIChE J.*, 1, (1955), 4, pp. 531–535, doi: 10.1002/aic.690010425.
- [32]Pioro, I. L., et. al., Nucleate pool-boiling heat transfer. II: assessment of prediction methods, *Int. J. Heat Mass Transf.*, 47, (2004), 23, pp. 5045–5057, doi: 10.1016/j.ijheatmasstransfer.2004.06.020.
- [33]Jones, B. J., et. al., The Influence of Surface Roughness on Nucleate Pool Boiling Heat Transfer, *J. Heat Transf.*, 131,(2009), 121009, doi: 10.1115/1.3220144.
- [34]Cooper, M. G., Saturation Nucleate Pool Boiling - A Simple Correlation, *First U.K. National Conference on Heat Transfer*, 2.86, (1984), pp. 785–793. doi: 10.1016/B978-0-85295-175-0.50013-8.
- [35]Moffat, R. J., Describing the uncertainties in experimental results, *Exp. Therm. Fluid Sci.*, 1, (1988), 1, pp. 3–17, doi: 10.1016/0894-1777(88)90043-X.

Submitted: 27.6.2023.

Revised: 22.8.2023.

Accepted: 25.8.2023.